Towards Automated Reporting and Visualization of Lymph Node Metastases of Lung Cancer

Nico Merten[1,2], Philipp Genseke[3], Bernhard Preim[1,2], Michael C. Kreissl[1,3], Sylvia Saalfeld[1,2]

[1]Research Campus STIMULATE
[2]Department of Simulation and Graphics, Otto-von-Guericke University
[3]Department of Radiology and Nuclear Medicine, University Hospital Magdeburg

To cite this version:

Merten, N., Genseke, P., Preim, B., Kreissl, M. C., Saalfeld, S. Towards Automated Reporting and Visualization of Lymph Node Metastases of Lung Cancer. In *Proc. of Workshop Bildverarbeitung für die Medizin (BVM)*. IN PRINT. Lübeck, Germany. 2019.

Abstract

For lung cancer staging, the involvement of lymph nodes in the mediastinum, meaning along the trachea and bronchi, has to be assessed. Depending on the staging results, treatment options include radiation therapy, chemotherapy, or lymph node resection. We present a processing pipeline to automatically generate visualization-supported case reports to simplify reporting and to improve interdisciplinary communication, e. g. between nuclear medicine physicians, radiologists, radiation oncologists, and thoracic surgeons. To evaluate our method, we obtained detailed feedback from the local division of nuclear medicine: Although patient-specific anatomy was not yet considered, the presented approach was deemed to be highly useful from a clinical perspective.

1 Introduction

Worldwide, lung cancer has the highest incidence and mortality rates [Bray et al., 2018]. Popper [Popper, 2016] reports that depending on the type of lung carcinoma, cancer cells can migrate via blood vessels and cause distant metastases in the brain, bones, and the adrenal glands. Furthermore, they can also migrate via the lymphatic system and cause lymph node metastases.

In addition to the direct assessment of lung carcinomas, e. g. measuring their size and examining their shape, and whether distant metastases are present, the involvement of the mediastinal lymph nodes has to be taken into consideration in order select the right treatment option for the individual patient. Mountain et al. [Mountain and Dresler, 1997] introduced a "*Lymph Node Map*" that enables a uniform classification for lung cancer staging by grouping lymph nodes into *Lymph Node Stations*. Multiple extensions and variations of this classification exist. For example, Rusch et al. [Rusch et al., 2009] decreased the classification granularity by grouping stations into *zones*.

We present our processing pipeline that automatically generates case reports (see Fig. 1). Our approach is related to the *Tumor Therapy Manager* by Rössling et al. [Rössling et al., 2011], which examines lymph node levels to support treatment planning for cases with head and neck cancer. Additionally, it is also related to the tool of Birr et al. [Birr et al., 2011], which creates interactive oncology reports for the

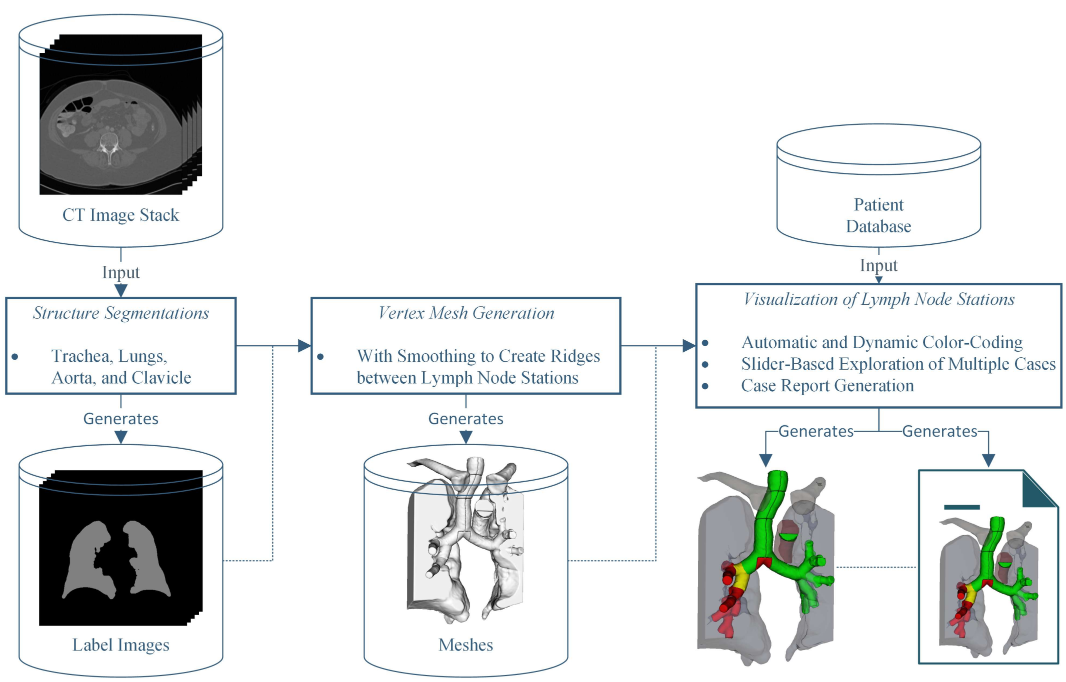

Figure 1: A detailed overview of the processing pipeline to generate visualization-supported case reports for lymph node metastases for lung cancer staging.

operation planning of lung tumors. Here, reports are used to document medical findings, and to support interdisciplinary communication between physicians that make diagnoses and surgeons, e. g. to plan lymph node resections.

2 Materials and Methods

The processing pipeline was implemented using *MeVisLab 2.8.2* [Ritter et al., 2011] and a detailed overview of the pipeline is depicted in Figure 1.

Structure Segmentation. For the first step, a *Computed Tomography* (CT) scan is used to create initial segmentation masks for important anatomical structures, namely the trachea, both lungs, the aorta, and the clavicle, which are then used to define lymph node stations. Considered stations, their anatomical location, and how they are geometrically encoded in the resulting visualizations and case reports are compiled in Table 1.

To obtain these segmentation masks, a region-growing approach with manual seed point definition was used. This is possible since the radio densities of the aforementioned and nearby structures are different enough to prevent an over-segmentation. However, to create lymph node stations, further processing was necessary (cf. Fig. 1 and 2). For our results, this was done manually: Starting a region-growing in the aortic arch included large parts of the heart, ascending arteries, and the abdominal aorta. Therefore, the aorta's segmentation mask was *cut* by defining clipping planes to exclude not needed anatomy. Two additional planes were then used to separate station 5 from the aorta.

All other stations are geometrically encoded using the trachea surface mesh. First, to separate the left and right lymph node stations, the segmentation mask was divided in the middle from the top to the carina. This processing step was automated by computing the axis-aligned bounding box for each axial slice and separating the left and right half. The horizontal *cuts* were also done manually using the vertical center of the clavicle (stations 1 and 2) and the upper edge of the aortic arch (stations 2 and 4). In Figure 2, this is depicted in detail. To separate the stations 10, 11 and 12, the skeletonization method of Selle et al. [Selle et al., 2002] was used, which is implemented in the *DtfSkeletonization* module in MeVisLab and resulted in a directed graph with the root node at the top of the trachea. While graph nodes represent airway branching points, graph edges represent the intermediate airways between these points. The airways behind the first bifurcation that divides the trachea into the primary bronchi are assigned to the stations 4L and 4R. Near the hilum, the primary bronchi are divided to separate the stations 4 and 10 from each other. The subsequent edges are assigned to the stations 10 (primary bronchi near hilum to lobar bronchi), stations 11 (lobar bronchi), and stations 12 (subsequent bronchi after lobar bronchi). Finally, to create station 7 at the bifurcation of the trachea, clipping planes were used to create the upside down, saddle-like geometry.

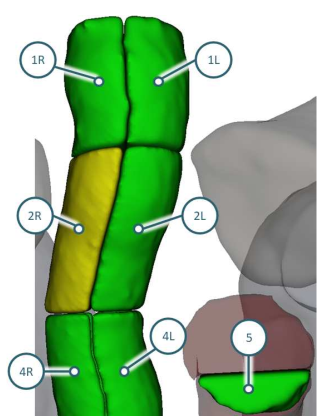

Figure 2: A focused depiction of the lymph node stations 1L/R, 2L/R, 4L/R, and 5 (cf. Tab. 1).

Table 1: Used lymph node stations, their anatomical location, and how they are geometrically encoded in the visualizations and case reports. The anatomical directions sinistra (left) and dextra (right) are abbreviated with L and R, respectively.

Lymph Node Station	Anatomical Location	Geometric Encoding
1L & 1R	Supraclavicler	Trachea, above clavicler
2L & 2R	Upper Paratracheal	Trachea, above aortic arch
4L & 4R	Lower Paratracheal	Rest of Trachea until Hilum
5	Subaortic	Segment at aortic arch
7	Subcarinal	Trachea, just above carina
10L & 10R	Hilum	Primary bronchi near Hilum
11L & 11R	Interlobar	Near Hilum to lobar bronchi
12L & 12R	Lobar	Subsequent bronchi

Although no lymph node stations were encoded using the lung parenchyma, it was segmented and visualized to create a visual context for the airways. However, segmenting the lung parenchyma via region-growing results in holes due to a rather high contrast between parenchyma and blood vessels. Therefore, a morphological closing operator was applied to close major holes.

Vertex Mesh Generation. For each segmentation mask, a surface mesh is generated using the *Neighboring Cells Algorithm* of Bade et al. [Bade et al., 2007], which is implemented in the *WEMIsoSurface* module in MeVisLab. After mesh generation, the Laplacian mesh smoothing from the *WEMSmooth* module is applied to all meshes to reduce staircase artifacts and to enhance the visual separation between adjacent lymph node stations by creating ridges along mesh borders.

3 Results

In the last processing step, the previously created meshes are visualized and color-coded (see Fig. 4). To create the color-coding, the user has to import a patient database with one or multiple cases that include the patient name, gender, and the individual metastases findings for each lymph node stations. We used

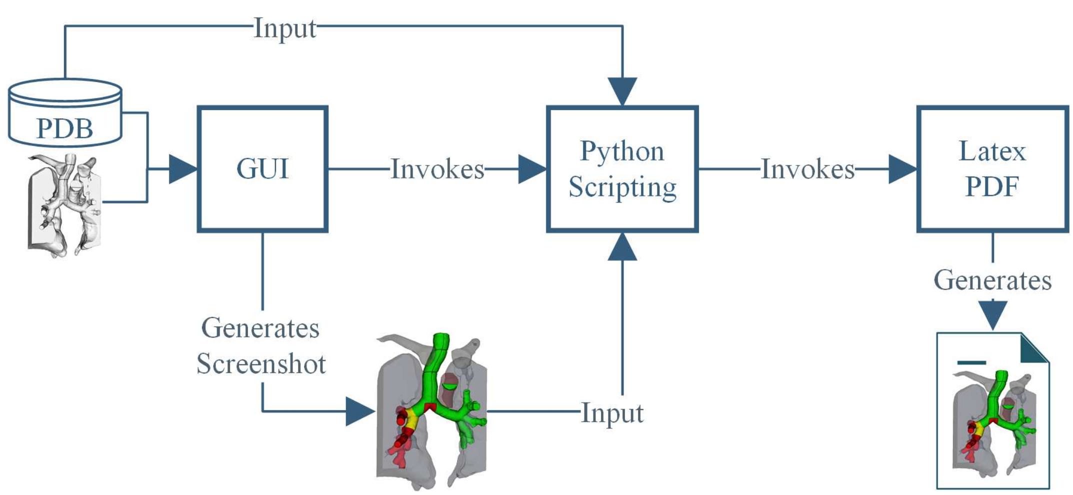

Figure 3: A detailed overview of the case report generation pipeline. A sreenshot of the 3D visualization is merged with patient information and individual lymph node metastases findings from the *Patient Database* (PDB; cf. Fig. 1). All information are collected via Python scripting and are then compiled in a case report via LaTeX.

the *Comma-Separated Values* (CSV) file format, because it can easily be generated and processed. Using the slider at the top right, users can interactively browse through all imported patients and the color-coding is adapted with respect to a patient's individual findings. Additionally, the color-coding for the lymph node stations and anatomic landmarks can be changed. Furthermore, the opacities of the landmarks can be changed interactively. To do that, the *Order-Independent Transparencies* method of Barta et al. [Barta et al., 2011] was implemented.

At the bottom right, users can export screenshots of the rendering canvas on the left and automatically generate case reports in the *Portable Document Format* (PDF) by defining an export path. The internal case report generation pipeline is depicted in Figure 3: Information about the patient and a screenshot of the currently presented 3D visualization are collected and merged via Python scripting in a LaTeX source file. When all information are present, a PDF case report is generated by invoking a LaTeX program, e. g. `pdflatex`.

4 Discussion

To evaluate our developed method, we received detailed feedback from our local division of nuclear medicine. First, the clinical suitability of the presented geometric encoding of lymph node stations was assessed. On the one hand, it was noted that the current approach introduces a rather high degree of anatomical abstraction, because lymph nodes are separate anatomic structures, but at this moment, they are represented via tracheal mesh geometry (cf. Table 1). On the other hand, the current approach was found to be easy to understand as well as to make clinical reports more straightforward to interpret.

For now, obtaining the initial segmentation masks and separating them into lymph node stations

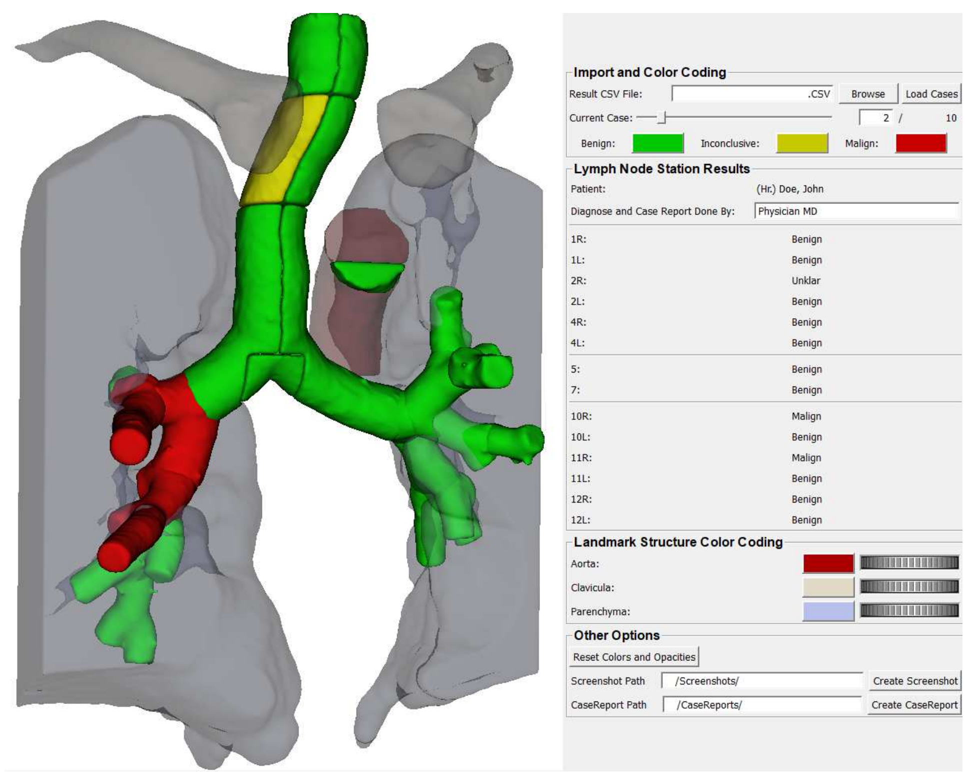

Figure 4: The *Graphical User Interface* with the resulting lymph node station visualization. On the right, the color-coding of the stations and anatomic landmarks can be changed. Furthermore, the individual metastases findings are presented in a list. At the bottom right, users can export automatically generated case reports (cf. Fig. 3).

was done manually. Our clinical cooperation partners stated that segmenting patient-specific anatomy for each new case would be too time-consuming in a clinical workflow, however, it was also mentioned that, currently, this was not necessary. Although this is not a favorable condition, it can be argued that always using the already obtained set of segmentation masks and surface meshes can be an advantageous, because the resulting case reports are uniform and comparable to each other. Moreover, this increases the familiarity with visualization-supported reports.

For lung cancer staging, our clinical colleagues use combined PET/CT scans with the F18-FDG radionuclide, which are not used in the current processing pipeline. Related to the *Tumor Therapy Manager* by Rössling et al. [Rössling et al., 2011], it would be desirable to extend the presented pipeline towards a *Computer-Assisted Diagnosis* prototype, which enables an automatic derivation of staging suggestions from suspicious metabolic activity of lymph nodes. Currently, users are required to create and maintain an additional database with individual lymph node metastases findings, however, this can easily be done using table processing software. Furthermore, regarding different staging classifications, e. g. by Mountain or Rusch et al. [Mountain and Dresler, 1997, Rusch et al., 2009], the presented processing pipeline and GUI can easily be adapted, which enables fast software tailoring for different clinical workflows. Finally, we searched for potential clinical applications areas with our cooperation partners: From the clinical point of view, resulting visualization-supported reports are seen as a very helpful addition for interdisciplinary communication scenarios, e. g. tumor board reviews, the planning of lymph node resections, or for the documentation in the context of clinical trials.

Acknowledgments

This work is partly funded by the Federal Ministry of Education and Research within the Forschungscampus *STIMULATE* (Grant Number 13GW0095A).

References

[Bade et al., 2007] Bade, R., Konrad, O., et al. (2007). Reducing Artifacts in Surface Meshes Extracted from Binary Volumes. *J WSCG*, 15(1-3):67–74.

[Barta et al., 2011] Barta, P., Kovács, B., et al. (2011). Order Independent Transparency with Per-Pixel Linked Lists. *Budapest University of Technology and Economics.*

[Birr et al., 2011] Birr, S., Dicken, V., et al. (2011). 3D-PDF: Ein interaktives Tool für das onkologische Reporting und die Operationsplanung von Lungentumoren. In *CURAC*, pages 11–16, Magdeburg.

[Bray et al., 2018] Bray, F., Ferlay, J., et al. (2018). Global Cancer Statistics 2018: GLOBOCAN Estimates of Incidence and Mortality Worldwide for 36 Cancers in 185 Countries. *CA Cancer J Clin.*

[Mountain and Dresler, 1997] Mountain, C. F. and Dresler, C. M. (1997). Regional Lymph Node Classification for Lung Cancer Staging. *Dis Chest*, 111(6):1718–1723.

[Popper, 2016] Popper, H. H. (2016). Progression and Metastasis of Lung Cancer. *Cancer Metastasis Rev*, 35(1):75–91.

[Ritter et al., 2011] Ritter, F., Boskamp, T., et al. (2011). Medical Image Analysis. *IEEE Pulse*, 2(6):60–70.

[Rössling et al., 2011] Rössling, I., Dornheim, J., et al. (2011). The Tumor Therapy Manager - Design, Refinement and Clinical Use of a Software Product for ENT Surgery Planning and Documentation. In *IPCAI*, pages 1–12.

[Rusch et al., 2009] Rusch, V. W., Asamura, H., et al. (2009). The IASLC Lung Cancer Staging Project: A Proposal for a New International Lymph Node Map in the Forthcoming 7th Edition of The TNM Classification for Lung Cancer. *J Thorac Oncol*, 4(5):568–577.

[Selle et al., 2002] Selle, D., Preim, B., et al. (2002). Analysis of Vasculature for Liver Surgical Planning. *IEEE Trans Med Imaging*, 21(11):1344–1357.